stage of study of such systems, the exchange formulation of the perturbations has been very useful.

Registry No. $Ru(NH_3)_6{}^{3+}Cl^-$, 53293-35-9; $Ru(NH_3)_6{}^{3+}Br^-$, 53293-36-0; $Ru(NH_3)_6{}^{3+}NCS^-$, 91760-60-0; $Ru(NH_3)_6{}^{3+}I^-$, 53293-37-1; $Co(H_2O)_6{}^{3+}$, 15275-05-5; $Co(H_2O)_6{}^{3+}Cl^-$, 91760-61-1; $Co(H_2O)_6{}^{3+}Br^-$, 91760-62-2; $Co(H_2O)_6{}^{3+}NCS^-$, 91760-63-3; $Co((bzo)_3[12]hexaeneN_3)_2{}^{3+}$, 47872-01-5; $Co((bzo)_3[12]hexaeneN_3)_2{}^{3+}I^-$, 91839-93-9; $Co((bzo)_3[12]hexaeneN_3)_2{}^{3+}NO_2{}^-$, 91839-94-0; $Co((bzo)_3[12]hexaeneN_3)_2{}^{3+}NCS^-$, 91839-95-1; $Co((bzo)_3[12]hexaeneN_3)_2{}^{3+}X^-$ (X^- = ascorbate), 91839-96-2; $Co(phen)_3{}^{3+}$, 18581-79-8; $Co(phen)_3{}^{3+}I^-$, 31415-56-2; $Co(phen)_3{}^{3+}NO_2{}^-$, 86176-93-4; $Co(phen)_3{}^{3+}Cl^-$, 86163-76-0; $Co(phen)_3{}^{3+}NCS^-$, 68369-95-9; $Co(phen)_3{}^{3+}NCS^-$, 68369-95-9; $Co(phen)_3{}^{3+}X^-$ (X^- = ascorbate), 86163-74-8; $Fe(phen)_3{}^{2+}$, 14708-99-7; $Co(sep)^{2+}$, 63218-22-4; $Co([9]aneN_3)_2{}^{2+}$, 91760-59-7.

Supplementary Material Available: Tables of pseudo-first-order rate constants (7 pages). Ordering information is given on any current masthead page.

Contribution from the Departments of Chemistry and Physics, Karl Marx University, DDR-7010 Leipzig, GDR, and Department of Molecular Spectroscopy, University of Nijmegen, 6525 ED Nijmegen, The Netherlands

Single-Crystal ^{13}C ENDOR and TRIPLE Resonance Studies on Tetra-*n*-butylammonium Bis(*cis*-1,2-dicyanoethenedithiolato)cuprate(II), $(n\text{-}Bu_4N)_2[Cu(mnt)_2]$

R. KIRMSE,[*,†] J. STACH,[†] U. ABRAM,[†] W. DIETZSCH,[†] R. BÖTTCHER,[‡] M. C. M. GRIBNAU,[§] and C. P. KEIJZERS[*,§]

Received February 23, 1984

A single-crystal ENDOR study of tetra-*n*-butylammonium bis(*cis*-1,2-dicyanoethenedithiolato)cuprate(II), $(n\text{-}Bu_4N)_2[Cu(mnt)_2]$, is reported. The hyperfine tensors of all ^{13}C nuclei of the complex anion were evaluated. With TRIPLE resonance experiments the signs of the hyperfine couplings could be determined. The coupling constants could be understood with the aid of spin densities, which were obtained from extended Hückel molecular orbital calculations. Especially the inclusion of two- and three-center contributions to these ligand hyperfine couplings but also the TRIPLE experiments are shown to be essential in order to be able to draw conclusions about the electronic structure and the symmetry of the "highly covalent" $[Cu(mnt)_2]^{2-}$ anion.

Introduction

Transition-metal dithiolene complexes have attracted the interest of EPR spectroscopists already for many years because of (i) the high covalency of the metal–sulfur bonds, which is the cause of a large delocalization of the unpaired spin density, (ii) the different metal oxidation states that are stabilized by these ligands and result in various electronic configurations, (iii) the interesting behavior with respect to ligand-exchange reactions, and (iv) the ability to form one-dimensional systems and π-donor–acceptor complexes. Apart from the numerous EPR studies of dithiolene complexes in liquid or frozen solutions, to our knowledge more than 20 single-crystal EPR studies were reported, most of them[1-15] on homoligand complexes, some on donor–acceptor complexes,[16-18] and some on mixed-ligand systems with one dithiolene ligand.[19-23]

In order to characterize the bonding in detail, ligand hyperfine data are needed because they provide direct information about the nature of the electronic ground state and about the extent of electron-spin delocalization over the ligand orbitals. For dithiolene complexes it is very difficult to measure ligand hyperfine interactions with EPR because the only sulfur isotope with nonzero nuclear spin, ^{33}S, has a natural abundance of only 0.74%. Only in a few dithiolene complexes could ^{33}S hyperfine couplings (hfc's) be observed and analyzed.[2,9,11-13,21] The magnetic interactions of the other ligand nuclei–^{13}C, ^{14}N–are too weak to be resolved in the EPR spectra even if ^{13}C-enriched ligands are used.

In this paper we report a single-crystal ^{13}C ENDOR study on tetra-*n*-butylammonium bis(*cis*-1,2-dicyanoethenedithiolato)cuprate(II) (*cis*-1,2-dicyanoethenedithiolato is often called maleonitriledithiolato, mnt^{2-}), $(n\text{-}Bu_4N)_2[^{63}Cu(mnt)_2]$ (I), diamagnetically diluted by the corresponding nickel(II) complex, $(n\text{-}Bu_4N)_2[Ni(mnt)_2]$. The investigation of the ^{13}C hfc's was stimulated by the successful ^{13}C experiments that were recently carried out by us on the complex bis(diethyl-

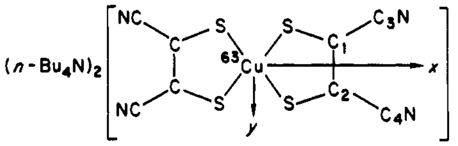

I

[†] Department of Chemistry, Karl Marx University.

[‡] Department of Physics, Karl Marx University.

[§] University of Nijmegen.

(1) Maki, A. H.; Edelstein, N.; Davison, A.; Holm, R. H. *J. Am. Chem. Soc.* **1964**, *86*, 4580.
(2) Schmitt, R. D.; Maki, A. H. *J. Am. Chem. Soc.* **1968**, *90*, 2288.
(3) Van Rens, J. G. M.; de Boer, E. *Mol. Phys.* **1970**, *19*, 745.
(4) Kwik, W.; Stiefel, E. I. *Inorg. Chem.* **1973**, *12*, 2337.
(5) Atherton, N. M.; Winscom, C. J. *Inorg. Chem.* **1973**, *12*, 383.
(6) Schlupp, R. L.; Maki, A. H. *Inorg. Chem.* **1974**, *13*, 44.
(7) Van Rens, J. G. M.; Viegers, M. P. A.; de Boer, E. *Chem. Phys. Lett.* **1974**, *28*, 104.
(8) Plumlee, K. W.; Hoffman, B. M.; Ibers, J. A.; Soos, Z. G. *J. Chem. Phys.* **1975**, *63*, 1926.
(9) Kirmse, R.; Dietzsch, W. *J. Inorg. Nucl. Chem.* **1976**, *38*, 255.
(10) White, L. K.; Belford, R. L. *J. Am. Chem. Soc.* **1976**, *98*, 4428.
(11) Kirmse, R.; Dietzsch, W.; Solovev, B. V. *J. Inorg. Nucl. Chem.* **1977**, *39*, 1157.
(12) Kirmse, R.; Stach, J.; Dietzsch, W.; Hoyer, E. *Inorg. Chim. Acta* **1978**, *26*, L53.
(13) Kirmse, R.; Stach, J.; Dietzsch, W.; Steimecke, G.; Hoyer, E. *Inorg. Chem.* **1980**, *19*, 2679.
(14) Duliba, E.; Seebauer, E. G.; Belford, R. L. *J. Magn. Reson.* **1982**, *49*, 507.
(15) Snaathorst, D.; Doesburg, H. M.; Perenboom, J. A. A. J.; Keijzers, C. P. *Inorg. Chem.* **1981**, *20*, 2526.
(16) Schmitt, R. D.; Wing, R. M.; Maki, A. H. *J. Am. Chem. Soc.* **1969**, *91*, 4391.
(17) Wing, R. M.; Schlupp, R. L. *Inorg. Chem.* **1970**, *9*, 471.
(18) Manoharan, P. T.; Noordik, J. H.; de Boer, E.; Keijzers, C. P. *J. Chem. Phys.* **1981**, *74*, 1980.
(19) Dietzsch, W.; Stach, J.; Kirmse, R. *Z. Chem.* **1977**, *17*, 191.
(20) Stach, J.; Kirmse, R.; Dietzsch, W.; Hoyer, E. *Inorg. Nucl. Chem. Lett.* **1978**, *14*, 143.
(21) Stach, J.; Kirmse, R.; Dietzsch, W. *Inorg. Chim. Acta* **1979**, *36*, L395.
(22) Kirmse, R.; Böttcher, R.; Keijzers, C. P. *Chem. Phys. Lett.* **1982**, *87*, 467.

0020-1669/84/1323-3333$01.50/0

dithiocarbamato)copper(II), $Cu(S_2CN(C_2H_5)_2)_2$.[24,25]

In the ENDOR spectra the signals of all carbon atoms of the complex anion were observed. In order to obtain an assignment of the ENDOR transitions to the correct C atoms, ENDOR spectra were also recorded for the same system but with the chelate ring atoms ^{13}C labeled.

To understand the bonding situation, the ^{13}C hfc tensors were also calculated by taking into account all two- and three-center contributions.[26] The MO coefficients that were used in these calculations were obtained from extended Hückel molecular orbital (EHMO) calculations. In order to be able to compare the calculated tensors with the experimental data, the absolute signs of the hfc data must be known. To obtain these signs, electron–nuclear–nuclear triple-resonance (TRIPLE) experiments were performed.

In addition to the ^{13}C ENDOR spectra, complicated ^1H ENDOR spectra were observed. Since the $[Cu(mnt)_2]^{2-}$ anion does not contain protons, these ^1H ENDOR transitions must be caused by intermolecular interactions with protons belonging to the $(n\text{-}Bu_4N)^+$ cations. The ^1H hfc's of some of the protons were studied because the knowledge of the directions of the maximum splitting of the nearest lying protons is necessary for the determination of the absolute signs in the TRIPLE experiments.

Experimental Section

A. Preparation of Complexes and Crystals. The ligand salt Na_2mnt was prepared according to the unique method of Bähr and Schleitzer;[27-29] see eq 1 and 2 (DMF = dimethylformamide).

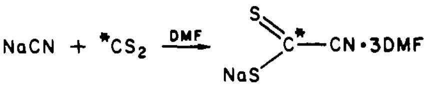

$$\mathrm{NaCN} + {}^{*}\mathrm{CS_2} \xrightarrow{\mathrm{DMF}} \mathrm{NaS}\overset{*}{\mathrm{C}}(\mathrm{=S})\mathrm{-CN\cdot 3DMF} \qquad (1)$$

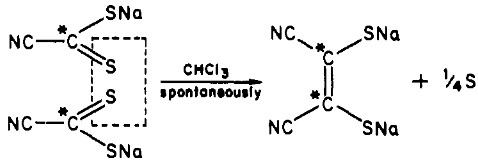

(2)

$(n\text{-}Bu_4N)_2[^{63}Cu(mnt)_2]$ and $(n\text{-}Bu_4N)_2[Ni(mnt)_2]$ were obtained as described in ref 30. For the preparation of the copper complex, ^{63}Cu-enriched $CuCl_2{\cdot}2H_2O$ was used (97.8% ^{63}Cu, 2.2% ^{65}Cu).

The syntheses of the ^{13}C-labeled complexes were performed in the same way by using ^{13}C-enriched CS_2 (enrichment 35%), which was prepared from $Ba^{13}CO_3$ as described in ref 31. According to eq 1 and 2, in this way mnt complexes can be prepared in which only the chelate ring atoms are ^{13}C labeled (labeled C atoms are marked by asterisks).

Platelike single crystals containing 0.1–0.5 mol % $(n\text{-}Bu_4N)_2[^{63}Cu(mnt)_2]$ in the corresponding diamagnetic Ni(II) complex were grown by slow solvent evaporation from acetone/ethanol (4:1) solutions. The dimensions of the crystals which were used in the ENDOR/TRIPLE experiments were about 2 × 5 × 5 mm.

B. EPR–ENDOR–TRIPLE Measurements. EPR spectra were recorded at $T = 295$ and 27.2 K on a Varian E 112 spectrometer at X-band frequency.

The ENDOR investigations were made with a modified Varian E 1700 spectrometer at $T = 27.2$ K using liquid neon. This low-power ENDOR apparatus employs a 20-W distributed amplifier, which is loaded by a three-turn coil placed inside the H_{102} cavity. The measurements were done in the differential mode (Δf mode) without low-frequency magnetic field modulation. The radio frequency range available for studying the ENDOR transitions was 0.5–130 MHz.

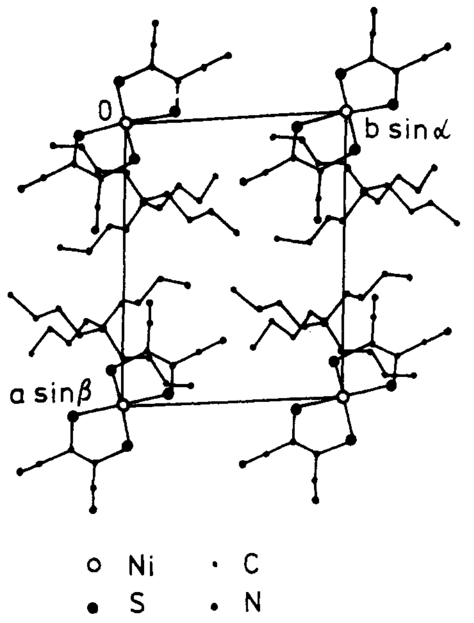

Figure 1. Projection in the *bc* plane of the structure of the host crystal $(n\text{-}Bu_4N)_2[Ni(mnt)_2]$.[32]

Table I. Principal Values of the g Tensor and the ^{63}Cu Hfc Tensor at $T = 27.2$ K and at Room Temperature[a]

	$T = 27.2$ K[b]	room temp[c]
g_x	2.020	2.023
g_y	2.023	2.026
g_z	2.089	2.086
A_x	−43.1	−39.0
A_y	−43.7	−39.0
A_z	−171.4	−162.0
$\langle A_{av} \rangle$	−86.1	−80.0

[a] Hyperfine couplings are in units of 10^{-4} cm^{-1}. [b] This work. Experimental errors: g_i, ±0.001; A_i, ±0.3 ($i = x, y, z$). [c] Data taken from ref 1.

The angular dependence of the EPR–ENDOR spectra was measured in the molecular plane that is the plane of the smallest *g* anisotropy (*xy* plane) and in two planes perpendicular to the *xy* plane (thus containing the *z* axis). ENDOR spectra were recorded every 5 or 10°, depending on their complexity.

For the electron–nuclear–nuclear triple-resonance experiments, the E 1700 ENDOR spectrometer is supplemented by an rf generator and a tunable power amplifier with a maximal output of about 40 W. The frequency range of this ENDOR system is 3–40 MHz. Also in the TRIPLE experiments a H_{102} cavity was used. Inside this cavity, two flat rf coils with three turns are placed in a plane in which the electric field is zero.

Experimental Results

A. EPR Spectra. The crystal structures of $(n\text{-}Bu_4N)_2[Ni(mnt)_2]$[32] and $(n\text{-}Bu_4N)_2[Cu(mnt)_2]$[8] are known. Both crystallize in the triclinic space group $P\bar{1}$ with $Z = 1$. A projection of the structure of the former compound as viewed along the *c* axis is shown in Figure 1. The anion is nearly planar; the Ni atom occupies an inversion center. In contrast to the anions of $(n\text{-}Bu_4N)_2[Ni(mnt)_2]$, the $[Cu(mnt)_2]^{2-}$ anions crystallize in stacks, thus forming linear chains. In the anion $[Cu(mnt)_2]^{2-}$, the deviations from planarity are larger than those observed for $[Ni(mnt)_2]^{2-}$. Also, the two different metal–sulfur bond distances deviate more from each other.

The room-temperature single-crystal EPR spectra of $(n\text{-}Bu_4N)_2[Cu/Ni(mnt)_2]$ were investigated first by Maki et al.[1] Considerably later, the ^{63}Cu nuclear quadrupole[10] and ^{33}S

---

(23) Stach, J.; Kirmse, R.; Abram, U.; Dietzsch, W.; Noordik, J. H.; Spee, K.; Keijzers, C. P. *Polyhedron* **1984**, *3*, 433.

(24) Kirmse, R.; Abram, U.; Böttcher, R. *Chem. Phys. Lett.* **1982**, *88*, 98.

(25) Kirmse, R.; Abram, U.; Böttcher, R. *Chem. Phys. Lett.* **1982**, *90*, 9.

(26) Keijzers, C. P.; Snaathorst, D. *Chem. Phys. Lett.* **1980**, *69*, 348.

(27) Bähr, G.; Schleitzer, G. *Angew. Chem.* **1956**, *68*, 525.

(28) Bähr, G.; Schleitzer, G.; Bieling, H. *Chem. Tech. (Leipzig)* **1956**, *8*, 597.

(29) Bähr, G.; Schleitzer, G. *Chem. Ber.* **1957**, *90*, 438.

(30) Billig, E.; Williams, R.; Bernal, I.; Waters, J. H.; Gray, H. B. *Inorg. Chem.* **1964**, *3*, 663.

(31) Abram, U.; Kirmse, R.; Bubner, M. *Z. Chem.* **1982**, *22*, 216.

(32) Kobayashi, A.; Sasaki, Y. *Bull. Chem. Soc. Jpn.* **1977**, *50*, 2650.

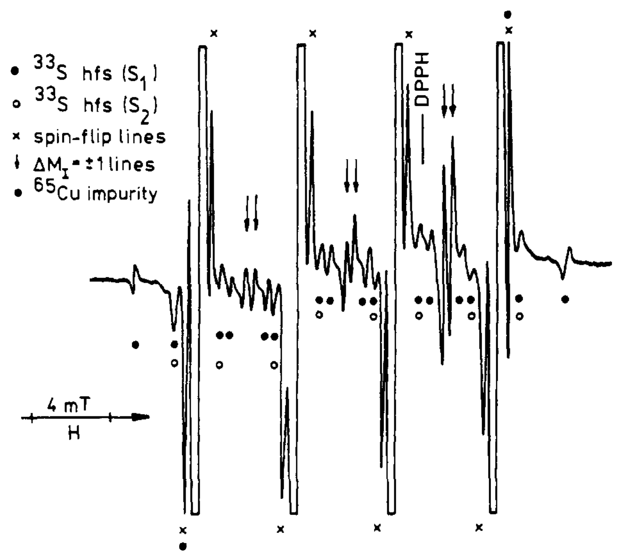

Figure 2. Typical room-temperature single-crystal EPR spectrum of $(n\text{-}Bu_4N)_2[^{63}Cu/Ni(mnt)_2]$ showing the ^{33}S satellite and proton spin-flip lines (^{63}Cu enrichment 97.8%).

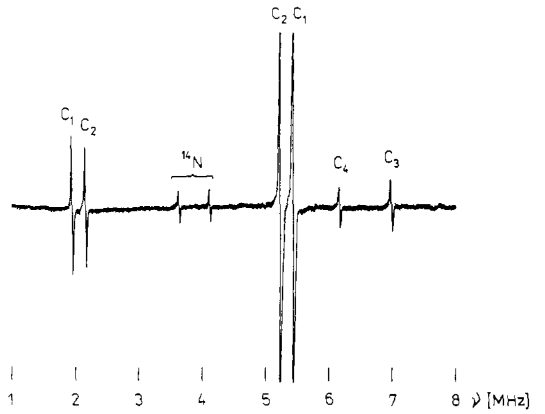

Figure 3. Typical single-crystal ^{13}C ENDOR spectrum of $(n\text{-}Bu_4N)_2[^{63}Cu/Ni(mnt)_2]$ at $T = 27.2$ K. The chelate ring carbon positions C_1 and C_2 are ^{13}C labeled (~35%).

ligand hfc's[12] were analyzed. The latter analysis shows the presence of two pairs of nonequivalent S atoms. Therefore, the inversion center of the $[M(mnt)_2]^{2-}$ unit is retained in the doped crystals. A typical EPR spectrum at $T = 295$ K with the ^{33}S satellite lines as well as proton spin–flip transitions is reproduced in Figure 2. The principal values of the **g** tensor and the ^{63}Cu hfc tensor $\mathbf{A}^{Cu}$ at $T = 27.2$ K are listed in Table I, together with the values measured by Maki et al.[1] at room temperature. The principal axes of the **g** tensor coincide with those of $\mathbf{A}^{Cu}$ at both temperatures.

There are some differences in the magnitudes of the principal values of $\mathbf{A}^{Cu}$ measured at $T = 295$ and 27.2 K: both the dipolar and the isotropic parts are somewhat larger at liquid-neon temperature. A similar result was obtained for the CuS_4 chelate bis(diethyldithiocarbamato)copper(II).[33] Since changes in the orientations of the principal axes of **g** and $\mathbf{A}^{Cu}$ were not observed, small changes in the bond lengths and/or angles within the coordination sphere must be responsible for the increase of the Cu hyperfine coupling parameters.

B. ^{13}C ENDOR Spectra. The ^{13}C ENDOR transitions were observed in the frequency range 1.5–7.0 MHz. A typical spectrum of the ^{13}C-enriched molecule is shown in Figure 3.

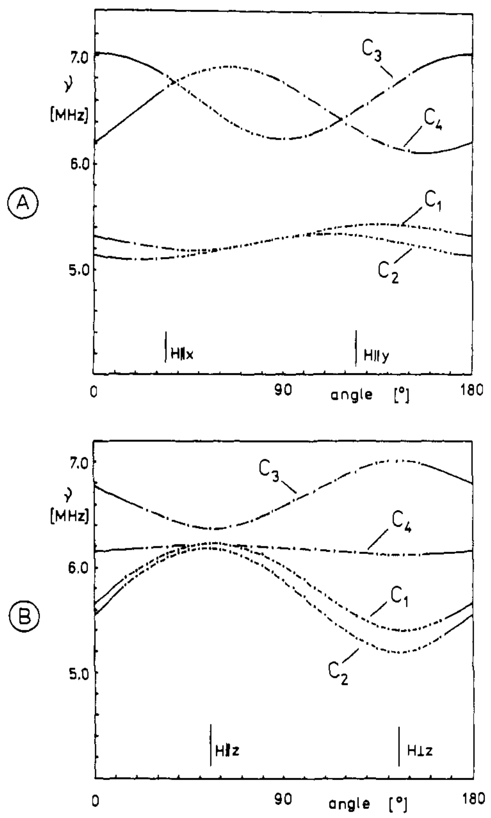

Figure 4. Angular variation of the ^{13}C ENDOR frequencies for (A) the molecular *xy* plane and (B) a plane that contains the molecular *z* axis. Part B intersects part A at 165°.

Each ^{13}C nucleus ($I = {}^1/_2$) gives rise to two ENDOR transitions with the first-order frequencies[34]

$$\nu^{(1)}(M_s) = \left|\left\{\tilde{\boldsymbol{l}}\widetilde{\left(\frac{1}{g}M_s\mathbf{g}\mathbf{A}^{C} - \nu_L^C\mathbf{1}\right)}\left(\frac{1}{g}M_s\mathbf{g}\mathbf{A}^{C} - \nu_L^C\mathbf{1}\right)\boldsymbol{l}\right\}^{1/2}\right| \tag{3}$$

where $g = |\{\tilde{\boldsymbol{l}}\cdot\mathbf{g}\cdot\tilde{\mathbf{g}}\cdot\boldsymbol{l}\}^{1/2}|$, $\nu_L^C = \mu_N g_C \boldsymbol{B}_0$ is the Larmor frequency of the ^{13}C nucleus, and **1** is the three-dimensional unit matrix. The orientation of the static field $\mathbf{B}_0$ with respect to the molecular coordinate system (defined in I) is indicated by the unit vector $\boldsymbol{l}$.

If the inversion center is retained in the Cu-doped molecules, 4 × 2 ^{13}C-ENDOR transitions are expected. The four high-frequency transitions could easily be observed, as may be concluded from Figure 3. Out of the corresponding low-frequency transitions, only those that belong to ^{13}C-enriched positions could be observed. Their intensity is drastically reduced with respect to the corresponding high-frequency lines. Therefore, these transitions could only be observed for C_1 and C_2 and not for C_3 and C_4. In addition, the C_3 and C_4 low-frequency transitions were outside the accessible frequency range for most of the crystal orientations because for these atoms $A/2$ is roughly equal to ν_L^C.

The line widths of the ^{13}C ENDOR lines were on the order of 20 kHz; the accuracy of the measured transition frequencies was about 5 kHz. The angular variations of the ENDOR frequencies in the coordination plane (molecular *xy* plane) and in a plane that contains the molecular *z* axis are shown in Figure 4. The ENDOR data were analyzed for each ^{13}C nucleus individually by using the spin Hamiltonian

$$H_{sp} = \mu_B \boldsymbol{B}_0\cdot\tilde{\mathbf{g}}\cdot\boldsymbol{S} + \boldsymbol{S}\cdot\tilde{\mathbf{A}}^{C}\cdot\boldsymbol{I} - g_C\mu_N\boldsymbol{B}_0\cdot\mathbf{I} \tag{4}$$

---

[33] Snaathorst, D.; Keijzers, C. P.; Klaassen, A. A. K.; de Boer, E.; Chacko, V. P.; Gomperts, R. *Mol. Phys.* **1980**, *40*, 585.

[34] Schweiger, A.; Graf, F.; Rist, G. H.; Günthard, Hs. H. *Chem. Phys.* **1976**, *17*, 155.

Table II. Experimental[a] and Calculated[b] Principal Values of the ^{13}C Hyperfine Splitting Tensors (in 10^{-4} cm^{-1}) and Direction of Their Principal Axes Relative to Those of the g Tensor

	calcd											
	STO		STO-5GTO first order[c]						exptl[d]			
						directions				directions		
atom	first order, one center	first and second order, one center	one center	two and three center	one, two, and three center = total	x	y	z	values	x	y	z
(i) Using Structure of $[Cu(mnt)_2]^{2-}$ [8]												
C_1 x	−0.067 (x, 38)	−0.068 (x, 33)	−0.066 (x, 45)	+0.331 (x, 3)	+0.334	11	96	81	+0.294	13	103	90
y	−0.068 (y, 33)	−0.060 (y, 15)	−0.066 (y, 30)	−0.026 (y, 3)	−0.081	82	13	101	+0.129	77	13	90
z	+0.135 (z, 33)	+0.128 (z, 34)	+0.131 (z, 33)	−0.305 (z, 2)	−0.254	98	78	14	−0.425	90	90	1
iso	0.675	0.679	0.492	0.085	0.577				−1.326			
C_2 x	−0.100 (x, 33)	−0.100 (x, 30)	−0.098 (x, 50)	+0.335 (x, 1)	+0.332	14	85	77	+0.311	15	75	90
y	−0.100 (y, 18)	−0.093 (y, 16)	−0.098 (y, 39)	−0.029 (y, 3)	−0.100	100	25	68	+0.138	105	15	90
z	+0.201 (z, 30)	+0.193 (z, 28)	+0.195 (z, 30)	−0.306 (z, 3)	−0.232	100	114	27	−0.448	90	90	2
iso	0.643	0.647	0.469	0.077	0.546				−1.270			
C_3 x	−0.368 (x, 30)	−0.381 (x, 32)	−0.358 (x, 29)	−0.075 (y, 36)	−0.184	175	86	94	−0.205	125	35	90
y	+0.737 (y, 21)	+0.745 (y, 21)	+0.717 (y, 22)	+0.190 (x, 11)	+0.630	85	21	110	+0.325	35	55	90
z	−0.369 (z, 37)	−0.363 (z, 38)	−0.358 (z, 34)	−0.116 (z, 34)	−0.445	92	70	21	−0.120	90	90	0
iso	1.406	1.403	1.026	0.102	1.127				+1.945			
C_4 x	−0.383 (x, 29)	−0.376 (x, 46)	−0.372 (x, 11)	−0.069 (y, 31)	−0.195	2	90	88	−0.219	118	152	90
y	+0.766 (y, 32)	+0.771 (y, 40)	+0.745 (y, 32)	+0.192 (x, 14)	+0.649	89	149	121	+0.326	28	118	90
z	−0.383 (z, 43)	−0.394 (z, 45)	−0.372 (z, 33)	−0.123 (z, 30)	−0.454	91	121	31	−0.106	90	90	0
iso	1.297	1.295	0.946	0.095	1.041				+1.854			
(ii) Assuming D_{2h} Symmetry												
C_1 x	+0.037 (x, 23)	+0.030 (x, 22)	+0.037 (x, 23)	+0.332 (x, 2)	+0.359	5	95	90	+0.294	13	103	90
y	−0.018 (y, 23)	−0.011 (y, 22)	−0.019 (y, 23)	−0.036 (y, 2)	−0.048	85	5	90	+0.129	77	13	90
z	−0.019 (z)	−0.019 (z)	−0.018 (z)	−0.296 (z)	−0.315	90	90	0	−0.425	90	90	1
iso	0.681	0.685	0.497	0.084	0.580				−1.326			
C_3 x	−0.291 (x, 1)	−0.297 (x, 1)	−0.283 (x, 1)	+0.181 (x, 11)	−0.117	174	84	90	−0.205	125	35	90
y	+0.583 (y, 1)	+0.591 (y, 1)	+0.567 (y, 1)	−0.087 (y, 11)	+0.495	84	6	90	+0.325	35	55	90
z	−0.292 (z)	−0.291 (z)	−0.284 (z)	−0.094 (z)	−0.378	90	90	0	−0.120	90	90	0
iso	1.393	1.391	1.016	0.103	1.119				+1.945			

[a] Experimental errors: A_i (i = x, y, z), ±0.010 (×10^{-4} cm^{-1}). [b] In parentheses is given the angle to the corresponding principal axis. [c] The first two columns list the principal values of the one- or the two- and three-center contributions to the hyperfine splitting tensor. For the calculation of the total principal values, these tensors were added and the total tensor was subsequently diagonalized. [d] Signs are obtained by the TRIPLE experiments.

In the analysis, interactions of the Cu nucleus (Zeeman, hyperfine, and quadrupole) were neglected. They contribute in second order to the ENDOR frequencies. Their omission is justified because the ENDOR frequencies obtained by saturating different Cu hyperfine lines in one EPR spectrum were identical after scaling to a constant magnetic field value.[33,35]

A Fortran IV computer program was written to calculate the elements of the symmetric tensors $\tilde{A}^C$ with the formalism given by Schweiger and Gunthard.[36] This program was linked to the minimization program MINUITS that minimizes the error function

$$h[N^{-1}\sum_{i=1}^{N}(\nu^{i}_{\text{obsd}} - \nu^{i}_{\text{calcd}})^2]^{1/2} \qquad (5)$$

The principal values of the ^{13}C hyperfine tensors and their directions relative to the axes of the molecular coordinate system (see I) are given in Table II.

As can be seen from Figure 3, in the frequency range of the ^{13}C lines some other ENDOR transitions were observed whose intensities depend strongly on the direction of $\boldsymbol{B}_0$. These are caused by long-range interactions with the ^{14}N nuclei of the cyano groups of the ligands and appear to be mainly determined by ^{14}N quadrupole interactions ($|P^N| > |A^N|$). A similar ^{14}N ENDOR pattern was observed for several other CuS_4 complexes and will be analyzed in detail in a subsequent paper.[37]

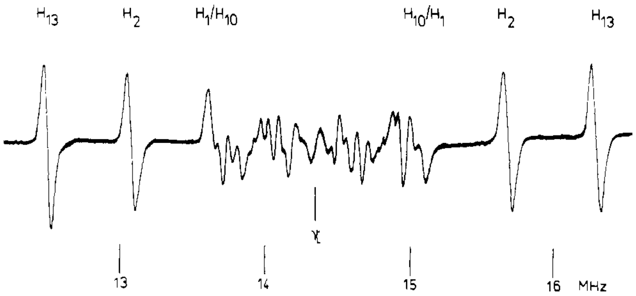

Figure 5. Typical single-crystal ^1H ENDOR spectrum of $(n\text{-}Bu_4N)_2[^{63}Cu/Ni(mnt)_2]$ at T = 27.2 K. The proton numbering corresponds to that given in ref 32.

C. ^1H ENDOR Spectra. The proton ENDOR spectra are very complex as can be seen from Figure 5, in which a typical one is shown. The complexity is due to the large number of $(n\text{-}Bu_4N)^+$ protons with a small distance to the Cu nucleus. The spectra of four protons were studied in detail.

The ^1H ENDOR data were treated in the same way as those for ^{13}C. The proton couplings determined are listed in Table III. In a point-dipole approximation the axial components of the hyperfine tensors are expected to be oriented along the Cu–H directions. Therefore, the assignment of the observed proton transitions was made with the aid of the direction cosines of the Cu–H vectors as calculated from the crystallographic data. The directions of the calculated Cu–H vectors

---

(35) Kita, S.; Hashimoto, M.; Iwaizumi, M. *Inorg. Chem.* **1979**, *18*, 3432.
(36) Schweiger, A.; Günthard, Hs. H. *Chem. Phys.* **1978**, *32*, 35.
(37) Böttcher, R.; Kirmse, R., to be submitted for publication.

Table III. Proton Hyperfine Coupling Parameters[a,b]

proton[c]	$10^4 A_{\parallel}^H$, cm^{-1}	directns of $A_{\parallel}^H$ g_x	g_y	g_z	directns of Cu-H[d] (X-ray data) g_x	g_y	g_z	dist of Cu-H (X-ray data),[d] Å
H_{13}	1.32	80	78	166	78	79	163	3.075
H_2	0.97	84	110	159	78	119	148	3.409
H_1	0.59	103	109	156	100	115	153	4.064
H_{10}	0.65	125	87	145	130	88	140	3.926

[a] The proton coupling tensors are considered to be determined by dipolar interaction exclusively (see text); therefore, only the axial components $A_{\parallel}^H$ are given. Direction cosines refer to the principal axes of the g tensor. [b] Experimental error: $A_{\parallel}^H$, $\pm 0.03 \times 10^{-4}$ cm^{-1}. [c] The proton numbering corresponds to that given by Kobayashi and Sasaki.[32] [d] Calculated from the structure of the Ni host complex.[32]

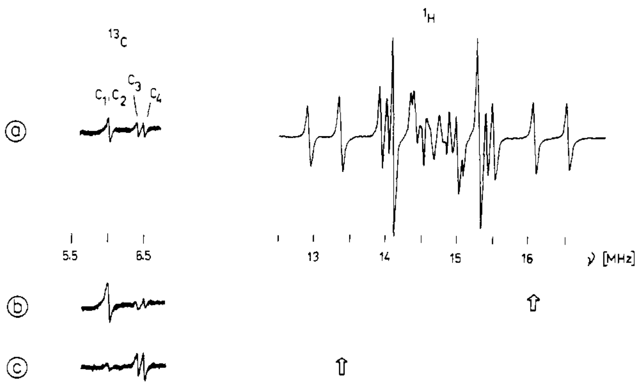

Figure 6. TRIPLE experiment for the determination of the signs of the carbon-13 hyperfine couplings. (a) ^{13}C (natural abundance) and ^1H ENDOR spectra. The chelate ring ^{13}C nuclei C_1 and C_2 are magnetically equivalent for this crystal orientation. (b) TRIPLE spectrum: saturated ^1H ENDOR transition, ν_+ (proton H_2) at 16.0 MHz; observer, ^{13}C ENDOR transitions. (c) TRIPLE spectrum: saturated ^1H ENDOR transition, ν_-(proton H_2) at 13.3 MHz; observer, ^{13}C ENDOR transitions.

deviated by not more than 10° from the experimental principal axes ($A_{\parallel}^H$).

D. TRIPLE Spectra. In this type of experiment, the intensity change of the ^{13}C ENDOR transitions is recorded as a function of a second radio frequency that is used to saturate the proton ENDOR lines of an exclusively dipolar-coupled proton in the region of its maximum hyperfine splitting ($\boldsymbol{B}_0 \approx\parallel A_{\parallel}^H$). This condition must be fulfilled because only for such an orientation is it allowed to assume that the sign of the proton coupling is positive. For the experiments, the protons H_2 and H_{13} were used (the numbering corresponds to that given by Kobayashi and Sasaki[32]).

Representative TRIPLE spectra are shown in Figure 6. Saturation of the high-frequency transition of the proton H_2 at 16.0 MHz resulted in an increase of the ENDOR intensity of the ^{13}C ENDOR line at 6.0 MHz assigned to the high-frequency transitions of C_1 and C_2 and in an intensity decrease of the ^{13}C high-frequency ENDOR lines at 6.4 and 6.5 MHz belonging to C_3 and C_4 (Figure 6b). This indicates that the resonances at 6.4 (6.5) and 16.0 MHz belong to the same M_s state. The transition at 6.0 MHz (C_1, C_2), however, belongs to the opposite M_s state. Since the proton coupling chosen has a positive sign, it follows that the couplings of C_3 and C_4 are positive and those of C_1 and C_2 are negative. This result was confirmed by the saturation experiment of the low-frequency transition of H_2 at 13.3 MHz (Figure 6c). In this case an intensity increase of the ENDOR lines at 6.4 and 6.5 MHz and a decrease of the ENDOR line at 6.0 MHz were observed.

It should be noted, that for the TRIPLE experiments a direction of $\boldsymbol{B}_0$ was chosen in which C_1 and C_2 are magnetically equivalent in order to increase the ENDOR signal intensity. The TRIPLE experiments were made on crystals with ^{13}C in natural abundance!

E. Computation of the ^{13}C Coupling Tensors. In this section the results are presented that were obtained for the carbon hfc tensors from calculations that include all one-, two-, and three-center contributions. The method used to calculate the ^{13}C tensors was described in detail in the literature.[26] The following steps have to be performed: (i) transformation of the coefficients of the (double-ζ) tesseral d functions of copper (as obtained from an extended Hückel calculation) into coefficients of Cartesian d functions, (ii) expansion of the single-ζ, non-core-orthogonalized Slater-type orbitals (STO's) (s and p orbitals in the basis set of the extended Hückel calculation) to double-ζ, core-orthogonalized STO's, retaining the Hückel MO coefficients for these extended STO's, and (iii) expansion of each STO into a linear combination of five Gaussian-type orbitals (GTO's) and substitution of these expansions into the MO of the unpaired electron.

In order to calculate the more-center contributions in the expression for the element ij of the hfc tensor of the nucleus N, given in eq 6, use was made of the property package of the

$$A^N_{ij} = \frac{\mu_0}{4\pi}\left\{g_e g_N \mu_B \mu_N \left[\left\langle \psi_0 \left| \frac{F^N_{ij}}{r_N^3} \right| \psi_0 \right\rangle + \frac{8\pi}{3}\langle \psi_0|\delta(r_N = 0)|\psi_0\rangle\right]\right\} \quad (6)$$

program POLYATOM.[38] Equation 6 represents the dipolar interaction between the spins of the unpaired electron and of the nucleus and the Fermi contact interaction. In eq 6, μ_0 is the permeability of free space and F^N_{ij} is an element of a symmetrical traceless tensor operator, centered on the nucleus N. ψ_0 is the MO of the unpaired electron, which is expanded as a linear combination of atomic orbitals, giving rise to the multicenter terms. All other symbols have their usual meaning.

In the calculations, all second-order contributions to the anisotropic hfc's were neglected. This neglect would be serious for the central metal hyperfine coupling,[39] but it is not for the ligand nuclei (sulfur, carbon).[26,40]

Two calculations were performed: for the first one the structure of the pure Cu complex (C_i symmetry) as determined by Soos et al.[8] was used; for the second one a structure with D_{2h} symmetry was assumed. For the latter structure the atomic coordinates were derived from the structure of the pure Cu complex by keeping as close as possible to the atom–atom distances.

The LCAO coefficients in the molecular orbital of the unpaired electron and the atomic spin density are listed in Table IV. The calculated ^{13}C tensors are presented in Table II. The tensors were also calculated with the previously described method[40,41] in which STO's are used but only one-center contributions are taken into account. In this way the reliability of the STO–GTO expansion can be tested by comparing these results with the one-center contribution as calculated with the GTO's. From Table II it may be concluded that this expansion is justified.

Discussion

In the ^{13}C ENDOR spectra the transitions of four different C atoms were observed, indicating the presence of magnetically

---

(38) Neumann, D. B.; Basch, H.; Kornegay, R. L.; Snyder, L. C.; Moskowitz, J. W.; Hornback, C.; Liebmann, C. B. *QCPE* **1974**, *11*, 199.

(39) Keijzers, C. P.; de Boer, E. *J. Chem. Phys.* **1972**, *57*, 1277.

(40) Keijzers, C. P.; de Boer, E. *Mol. Phys.* **1975**, *29*, 1007.

(41) Keijzers, C. P.; de Vries, H. J. M.; van der Avoird, A. *Inorg. Chem.* **1972**, *11*, 1138.

Table IV. MO Coefficients of the Unpaired Electron and Spin Densities

	structure of $[Cu(mnt)_2]^{2-}$ [8]		structure with D_{2h} symm	
atom	coefficients	density	coefficients	density
Cu	$0.71xy$	0.4065	$0.72xy$	0.4189
S_1	$-0.14s + 0.32x + 0.24y + 0.03z$	0.1309	$-0.14s + 0.31x + 0.25y$	0.1314
S_2	$0.13s - 0.30x + 0.24y - 0.04z$	0.1273		
C_1	$-0.025s - 0.024x + 0.010y - 0.040z$	0.0024	$-0.026s - 0.023x + 0.010y$	0.0012
C_2	$0.025s + 0.027x + 0.010y + 0.050z$	0.0033		
C_3	$-0.037s + 0.002x + 0.104y - 0.041z$	0.0109	$-0.037s + 0.001x + 0.099y$	0.0088
C_4	$0.035s + 0.005x + 0.096y + 0.061z$	0.0114		
N_1	$-0.009s + 0.024x - 0.078y + 0.037z$	0.0051	$-0.009s + 0.024x - 0.074y$	0.0039
N_2	$0.009s - 0.029x - 0.072y - 0.051z$	0.0054		

equivalent pairs of C atoms in the $[Cu/Ni(mnt)_2]^{2-}$ anions. This confirms the presence of an inversion center found from structural studies on both the pure Cu[8] and the pure Ni[32] complexes. The question of whether the incorporated Cu complex does completely accept the structure of the host lattice or not will be discussed below by means of the results obtained from the calculations.

There are several interesting and unexpected experimental results:

(i) The isotropic hfc's of the cyano group C atoms (C_3 and C_4) are in absolute value considerably larger than those for the chelate ring C atoms C_1 and C_2.

(ii) The dipolar parts of C_3 and C_4 are smaller than those for C_1 and C_2. This was expected because of the larger distance of the former pair to Cu. However, from the Cu–C distances a larger difference between the dipolar parts of C_1 and C_2 and the dipolar parts of C_3 and C_4 was expected.

(iii) All four ^{13}C tensors are rhombic; the planes of largest anisotropy were observed approximately in the molecular *xz* plane for C_1 and C_2 and in the *xy* plane for C_3 and C_4. One of the principal axes of each ^{13}C tensor is parallel with the molecular *z* azis, within experimental error.

(iv) The TRIPLE experiment shows that the signs of the largest component of the chelate ring C hfc's are opposite to those of the couplings of the cyano groups: C_1 and C_2 "–"; C_3 and C_4 "+".

To understand these observations, the experimental ^{13}C couplings will be compared with calculated ones from EHMO spin densities. From Table II it is quite clear that the one-center contributions alone cannot reproduce the experimental tensors. Although the relative order of the (absolute value of the) isotropic hfc's of C_1 and C_2 and of C_3 and C_4 is correct, the anisotropic hfc's of C_1 and C_2 are too small (and have the wrong sign), and those of C_3 and C_4 are too large. This concurs with previous results that the one-center contributions do explain the hfc's of the central metal atom and of the atoms of the first coordination sphere for copper complexes with unsaturated dichalcogeno ligands[15,23,40–43] but not for ligand atoms at large distances.[26,33] As noted already, from a comparison between the one-center contributions it may be concluded that the STO-5GTO expansion works very well, except for the isotropic hfc's. The latter is not surprising, since it is well-known that Gaussian orbitals do not obey the correct cusp condition at the nucleus.[26]

All calculated tensors depend strongly on the molecular structure. Although neither the copper molecule nor the host nickel complex has D_{2h} symmetry, it is suggested by the experimental results that the guest molecule is close to this symmetry because each tensor has one principal axis along the molecular *z* axis and the tensors of C_1 and C_2 and also those of C_3 and C_4 do not differ much. The fact that the agreement of the calculated tensors with the experiment is better in D_{2h} symmetry than in the original structure of the copper complex suggests also that the guest molecule is forced into a higher symmetry than in its own structure. It was checked whether the copper–ligand distances have a great influence on the calculated results. For that purpose, a third calculation was performed, also with D_{2h} symmetry but with shorter Cu–S distances (2.17 Å instead of 2.27 Å, which is close to the Ni–S distances in the host structure). It turned out that the calculated **g** tensor is much worse in the third calculation and also that the ^{13}C tensors did not improve. Therefore, it was concluded that the Cu–S distances are not shortened by the doping into the nickel crystal and that they are close to the distances in the pure copper crystal.

For C_3 and C_4 the calculations predict the correct sign for the hfc's and, in agreement with the experiment, the "axial" component of both tensors is located in the molecular plane. It is concluded that this part of the molecular orbital of the unpaired electron is rather well reproduced by our calculations—the s density on C_3 and C_4 is ~25% underestimated and the p density is overestimated (30% in D_{2h} symmetry)—a result that is very satisfying for atoms at such a large distance form the paramagnetic center. The relatively large spin density on the CN groups corresponds with the "electron-withdrawing" property that is ascribed to these groups.

Close to the C_1–C_2 axis there is a nodal plane in the MO of the unpaired electron. This explains why for C_1 and C_2 the one-center contributions depend very critically on the structure but for any geometry they are smaller than the more-center contributions. Already before the TRIPLE experiments, it was predicted from these calculated results that the signs of the hfc's of C_1 and C_2 would be negative, because if they were positive, then the one-center contribution should dominate since the two- and three-center contributions yield a negative hfc along *z* (and the maximum and positive principal value in the molecular plane). But a dominating one-center contribution would mean a large spin density in p_z, which is only possible if the molecule is nonplanar. Since the latter was highly improbable, on the basis of the crystallographic structures, it was predicted and later confirmed that these hfc's would be negative. Although our spin-restricted calculations resulted in a correct prediction of the sign and yielded qualitative insight into the bonding in this complex, they were naturally not able to reproduce these negative hfc's quantitatively. For that purpose, spin-unrestricted calculations must be performed. Preliminary results of NDDO calculations confirm that spin polarization indeed is the mechanism that is responsible for the sign of the $C_{1,2}$ hyperfine couplings.[44]

Acknowledgment. We thank Dipl.-Ing. D. Heinhold (Department of Physics, Karl Marx University) for his help in performing the ENDOR–TRIPLE experiments.

Registry No. $(n\text{-}Bu_4N)_2[^{63}Cu(mnt)_2]$, 67269-51-6.

---

(42) Keijzers, C. P.; de Boer, E. *Mol. Phys.* **1975**, *29*, 1743.

(43) Attanasio, D.; Keijzers, C. P.; van de Berg, J. P.; de Boer, E. *Mol. Phys.* **1976**, *31*, 501.

(44) Stach, J.; Kirmse, R.; Böttcher, R.; Nieke, C.; Reinhold, J., to be submitted for publication.